Journal of Materials Science: Materials in Medicine (2020) 31:96
https://doi.org/10.1007/s10856-020-06441-2

TISSUE ENGINEERING CONSTRUCTS AND CELL SUBSTRATES

Original Research

The effects of oyster shell/alpha-calcium sulfate hemihydrate/platelet-rich plasma/bone mesenchymal stem cells bioengineering scaffold on rat critical-sized calvarial defects

Jinwu Wang[1,2] · Linzhen Xie[1,2] · Xingyu Wang[1,2] · Wenhao Zheng[1,2] · Hua Chen[1,2] · Leyi Cai[1,2] · Long Chen[1,2]

Received: 15 February 2020 / Accepted: 24 September 2020 / Published online: 31 October 2020

Abstract

Engineering scaffolds combining natural biomineral and artificially synthesized material hold promising potential for bone tissue regeneration. We fabricated a bioengineering scaffold, oyster shell (OS) and alpha-calcium sulfate hemihydrate (α-CSH) as scaffold, platelet-rich plasma (PRP) as provider of growth factors and bone mesenchymal stem cells (BMSCs) as seed cells, and determined it could be applied as a new type of bone graft substitutes by rat calvarial defects repairing experiment in vitro and in vivo. SEM showed that the mean diameter of the pores was about 150 μm with a range of 50–200 μm, and scaffold's porosity was ~27.4% by Archimedes' Principle. In vitro, Scaffold + BMSCs + PRP group presented a higher ALP activity compared with other groups by ELISA ($P < 0.05$). But the expression of OC was not detectable on day 4 or 8. The MTT assay showed that the relative cell number of BMSCs+PRP group increased significantly ($P < 0.05$). In vivo, the smallest defect area of skull and highest volume of regenerated new bone were observed in Scaffold + PRP + BMSCs group by X-ray and Micro-CT analysis ($P < 0.05$). And the similar results also were observed in HE and Masson staining. The immunohistochemistry staining for osteogenic marker proteins ALP and OC showed that the most obvious positive staining was observed in Scaffold + PRP + BMSCs group ($P < 0.05$). The expression of inflammatory markers IL-6 and TNF-α was the lowest in control group ($P < 0.05$). In conclusion, a bioengineering scaffold based on OS, created by simply combining α-CSH and PRP and implanting with BMSCs, could be clinically useful and has marked advantages as a targeted, off-the-shelf, cell-loaded treatment option for the bone healing of critical-size calvarial defects.

Abbreviation

oyster shell	(OS)
alpha-calcium sulfate hemihydrate	(α-CSH)
platelet-rich plasma	(PRP)
bone mesenchymal stem cell	(BMSC)
fetal bovine serum	(FBS)
phosphate buffer saline	(PBS)
alkaline phosphatase	(ALP)
osteocalcin	(OC)
enzyme linked immunosorbent assay	(ELISA)
hethylenediaminetetraacetic acid	(EDTA)
calcium sulphate dihydrate	(CSD)

1 Introduction

In the clinic, the reconstruction of critical-sized bone defect remains challenging in orthopedics [1]. Bone grafts, namely autografts, allografts, and bone graft substitutes, are widely used to replace bone losses after defects due to a variety of causes. In present period, autografts and allografts are still major graft means in clinical practice, but their own inevitable drawbacks such as donor-site morbidity and immunogenicity restrict the use of transplantation [2]. To search for faultless alternatives, transplantation of bone graft substitutes seems to be a promisingly approach. With intensive clinical demand, the search for satisfactory bone graft materials has become a rapidly expanding field [3]. An ideal bone graft material should provide the combination of mechanical strength, angiogenesis,

These authors contributed equally: Jinwu Wang, Linzhen Xie

Jinwu Wang and Linzhen Xie should be considered co-first authors.

✉ Long Chen
chenlongcl2019@163.com

[1] Department of Orthopaedics Surgery, The Second Affiliated Hospital and Yuying Children's Hospital of Wenzhou Medical University, NO.109, XueYuan West Road, Luheng District, Wenzhou, Zhejiang Province 325000, P.R. China

[2] Wenzhou Medical University, Wenzhou, Zhejiang, China

and osteogenesis. Though various products have entered the market, and much more materials are under research, no perfect one is able to meet all the clinical requirement demands up to now. Searching for graft substitutes has become one of the research hotspots in the field of orthopedics.

Based on the triangular concept within tissue engineering [4], the standard method of bone tissue engineering included three essential pillars: scaffolds, bioactive factors, and osteogenic cell populations [4, 5]. The combinations of these tissue engineering construct might possess suitable osteoconduction, osteoinduction, and osteogenesis [6].

An ideal scaffold would have moderate biocompatibility, biodegradability, porosity, and well mechanical properties. The oyster shell (OS) tissue is a hard tissue mainly composed of organic matrix-calcium carbonate [7], the structure of which is similar to mammalian bone tissue [8]. Previous studies have revealed the biocompatibility and biodegradability of nacre derived from OS [8]. Similar to mammalian bone, the favorable mechanical strength and resilience are ensured by the microstructure [9]. In addition, it is also reported with osteoinductive and osteoconductive capability [8, 10]. In vitro experiment, it has been demonstrated that when human osteoblasts cultured with moderate nacre, a complete sequence of bone formation could be reproduced [11]. Oyster shell is also rich in natural porous structure, which is essential for cells' growth, differentiation and proliferation. But the slow degradation speed and limited resorption might hinder its use as a type of scaffold [12]. Though some studies have shown its promising potential, OS remains an underexplored biomaterial.

For exceptional osteoconductivity, osteoinductivity, biocompatibility and biodegradability, alpha-calcium sulfate hemihydrate (α-CSH) is a sufficient bone substitute and has been widely used in clinics as a replacement for autogenous cancellous grafts [13, 14]. When meeting water, α-CSH will turned into calcium sulphate dihydrate (CSD), which has been used to manufacture calcium sulfate cement for bone graft substitute and bone augmentation [15]. But the single use of α-CSH has certain drawbacks, mainly the relatively fast degradation rate and partly low mechanical strength [16]. To complement each other, OS powder was combined with α-CSH in the ratio of 1:3 as the scaffold.

Platelet-rich plasma (PRP), a kind of enriched platelet suspension in plasma from whole blood [17], is considered the source of cytokines and growing factors, including platelet derived growth factor, transforming growth factor-β, bone morphogenetic protein 2, and insulin-like growth factor, et cetera [18]. It can be activated into gel state by addition of calcium chloride or thrombin [2]. The application of PRP could promote wound healing, bone tissue regeneration, and angiogenesis [19]. And several animal studies have demonstrated the healing efficacy of using PRP as one part of therapeutic agents in critical-size defects [8].

Bone mesenchymal stem cells (BMSCs) possess the multipotential ability of differentiating into bone, cartilage, stroma, and so on [20], which have been extensively applied in tissue engineering. It has long been proven that when mixed with bone materials, BMSCs could act as promoters of critical-size bone defects' regeneration [21].

Therefore, we chose OS with α-CSH as the scaffold, PRP as the provider of growth factors, and BMSCs as seed cells. We fabricated this substitute material and tried to determine if this kind of bioengineering scaffold could be applied as a new type of bone graft substitutes by rat calvarial bone defects repairing experiment.

2 Materials and methods

2.1 Fabrication and morphological observation of scaffolds

Fresh oysters (Fig. 1) weight around 100 g were bought from a local seafood shop and shells were separated out. Oyster shells were rinsed thoroughly with distilled water and left to dry off. Then shells were crushed into powder by electric grinder. After passing through 200 mesh sieve, the grain was controlled less than 200 meshes. The powder was soaked in 10% chloroform for 24 h and the suspension was stirred with a magnetic stirrer. After washed by deionized water, the powder was soaked with stir in 30% hydrogen peroxide for 24 h. After ultrasonic cleaning with deionized water, the OS powder was left to dry in a hot-air drying oven. Calcium sulfate was also sifted by 200 mesh sieve after milled. At room temperature, added 18 g OS powder and 6 g calcium sulfate (the mass ratio = 1:3) into 25 ml absolute alcohol. The suspension was stirred with a magnetic stirrer for 30 min and sonicated. Then the mixture was poured into cylindrical molds sized with 5 mm in diameter and 4 mm in high and next dried at 37 °C for 24 h. Finally, scaffold powder was separated from the mold, sealed and stored in 4 °C refrigerator for use. We chose the fourier transform infrared spectra (FT-IR), X-Ray fluorescence (XRF), and X-ray diffraction (XRD) with Cu radiation to examined scaffold powder. When meeting water, α-CSH would turn into CSD and solidified in few minutes. Thus,

Fig. 1 Appearance and morphology of oyster shell

once scaffold powder mixed with deionized water, the paste-like mixture should be immediately fixed on a circular copper plate. After that, the scaffold's surface was coated with a palldium-gold film using a rotating sputtering machine. Then, the pore size and microstructure of scaffold were observed by SEM. The porosity of scaffold was measured by Archimedes' Principle [22, 23] and calculated as following:

$$V_p = (W_2 - W_3 - W_S)/\rho e,$$

$$V_S = (W_1 - W_2 + W_S)/\rho e,$$

$$\text{Porosity}(\%) = V_p/(V_p + V_S),$$

V_p standed for the volume of scaffold pore, V_S standed for the volume of scaffolds, W_S was the quality of the scaffold, W1 meaned the weight of bottle filled with ethanol, W_2 was the weight of bottle including the ethanol and the scaffold and then the bottle was weighed (W_3) after taking out of the ethanol-saturated scaffold.

2.2 Degradation test in vitro

We prepared the simulated body fluid (SBF) by the method introduced by Kokubo [24]. The pre-prepared sample of the scaffold (Φ 5 mm × 3 mm) was soaked in SBF solution, and then the soaking solution was collected at each immersion time point. The pH value and Ca^{2+} concentration in the soaking solution obtained at each time point were determined by electrolyte-type pH meter (FE20K, Mettler Toledo, Switzerland) and inductively coupled plasma-atomic emission spectrometry (ICP-AES, Optima 2100, USA).

2.3 Preparation of platelet-rich plasma

An SD rats (392 g) was anesthetized with intraperitoneal injections of 1.2 ml 10% chloral hydrate. After shaving and disinfection, open the thoracic cavity to expose the heart, then use syringe to collect 8 ml blood from the heart. The blood was soon mixed with 2 ml 10% sodium citrate and shaked up. Poured into centrifuge tube, the blood was divided into two obvious layers after dimission at 200 g for 10 min. The upper yellow layer was then dimission at 250 g for 10 min, and the bottom liquid except precipitate was collected as PRP. Around 1 ml PRP was derived and stored at −70 °C.

2.4 Preparation of thrombin

A 3000U thrombin (T6021, Biotopped) was added into 3 ml 10% calcium chloride solution. Shake well before use.

2.5 Primary culture and expression of BMSCs

Bone marrow was harvested from bilateral femurs of a 3-week-old male SD rat. After executed with overdose of intraperitoneal chloral hydrate, bilateral femurs were stripped out and cut off. Bone marrow was flushed out with phosphate buffer saline, and filtered with 100 um filter. After centrifugation, precipitate was cultured in cell medium which contained 80% (w/w) DMEM (C11995500bt, Gibco), 20% FBS (16000-044, Gibco) and Penicillin-Streptomycin(100 U/ml, P1400, Solarbio) at a humidified atmosphere of 37 °C and 5% CO_2. The medium was replaced in the 5th day and the first subculture was carried out in the 9th day. Cells were passaged in vitro with trypsin enzyme-digesting technique (T1300, Solarbio) when expanded to 80% confluence. When the 5th generation of cells expanded to 90% confluence, cells were gathered with 0.25% trypsin (T1300, Solarbio). After counting, the BMSCs suspension was diluted to 1.0×10^6 cells/ml for use [25].

2.6 BMSCs' implantation to scaffold in vitro

Mixed up 3000 mg scaffold with 1 ml deionized water, and then paved 800 ul paste-like mixtures at each well's bottom of 24 well culture plates. After scaffolds solidification, added 1 ml osteoblast induction medium (100 U/ml penicillin-streptomycin, 80% DMEM, 20% FBS, 10 mmol/L beta sodium glycerophosphate and 1.0×10^{-7} mol/L dexamethasone) into each well. The group I ($n = 8$) was added 5ul BMSCs suspension (1.0×10^6/ml) into each well. The group II ($n = 8$) was added with 5ul BMSCs suspension (1.0×10^6/ml), 10 ul PRP and 2 ul thrombin in each well. The group III ($n = 4$) was added with 10 ul PRP and 2 ul thrombin in each well. The group IV ($n = 4$) received no further procedure. The 24 well culture plate was placed at a humidified atmosphere of 37 °C and 5% CO_2 for 4 days. All wells' supernatants were collected for ELISA determination of alkaline phosphatase (ALP), osteocalcin (OC), and all wells' medium were replaced with 1.3 ml culture medium. After another 4 days' continued culture, the supernatant of each well was respectively collected for ELISA determination of alkaline phosphatase (ALP) and OC using alkaline phosphatase assay kit (A059-2, NJJCBIO) and osteocalcin assay kit (ml002883, mlbio).

2.7 BMSCs' proliferation assay

In total, 1.0×10^6 cells/ml BMSCs were cultured with 100 ul culture medium (80% DMEM with 20% FBS) in each well of a 96 well culture plate at 37 °C and 5% CO_2 for 24 h. Then medium was aspirated. The medium of group A ($n = 8$) was composed of 1.0 ml FBS and 4.0 ml DMEM.

And the medium of group B ($n = 8$) was composed of 1.0 ml FBS, 4.0 ml DMEM, 25 ul PRP and 5ul thrombin. 100 ul medium with 10 ul MTT solution was added into each well. The 96 well culture plate was continued cultured at 37 °C and 5% CO_2 for 4 h. Next steps were strictly in accordance with the specification of MTT assay kit (top0109, biotopped). And we measured the absorbance of each well at 570 nm by enzymatic-reader.

2.8 Surgical procedure

In total, 32 SD rats (168 ± 9 g) were randomly divided into four groups in the ratio of 1:1:1:1 by means of random number table. After anesthetized with intraperitoneal injections of 10% chloral hydrate (0.5 g for each rat), Hairs on the roof of skull were shaved and the skin was disinfected by iodophor. Do 1.5 cm sagittal median incision on the top, stripped out soft tissues until the calvarial bone was completely exposed. And a hole with a diameter of 5 mm in was drilled using a hollow electron trephine bur under saline cooling irrigation in unilateral calvaria, avoiding the sagittal suture. The round bone slice was then removed by scalpel without injury to the dura mater. Surgical field was then thoroughly washed with warm physiological saline. Each defect in group I, II, and III was paved with 20 mg premixing mixture scaffold (Premixing mixture scaffold: Mix 1000 mg scaffold powder with 334 ul deionized water). Next, each defect in group I was filled with 5 ul PRP, 1 ul thrombin, and 24 ul BMSCs suspension; each defect in group II was filled with 5 ul PRP, 1 ul thrombin, and 24 ul cell medium without BMSCs; each defect in group III was filled with 30 ul cell mediu (Cell medium: DMEM containing 20% FBS. Mixtures were immediately used after mixed), and each defect in group IV was filled with nothing. Then soft tissues were repositioned and incisions were sewn up by 4-0 suture. All rats received daily intraperitoneal daily injection of 50,000U penicillin for 5 days after surgery.

2.9 X-ray analysis

After the 4th and 8th week of surgical operation, four rats were sacrificed by overdose of intraperitoneal chloral hydrate in each group respectively. The skull defect specimens were taken and fixed with 4% paraformaldehyde. After 48 h of fixation, specimens were harvested using 75% alcohol. We then radiographed each sample by digital X-ray machine (Kubtec Model XPERT.8; KUB Technologies Inc.) to monitor the treated area about the presence of the new bone and area of remaining skull defect at four and eight weeks after surgical operation. And image pro-plus 6.0 (Media Cybernetics, Inc., MD, USA) was used to measure and analyze the area of remaining skull defect.

2.10 Micro-CT analysis

At 8th week after operation, the skull defect specimens of rats were fixed with 4% paraformaldehyde at 37 °C for 48 h. Then, bone specimens, containing a hole of 5 mm in diameter, were analyzed by Micro-CT (MicroCTμ100, SCANCO Medical, Switzerland) scans. Skull specimens were scanned at 70 KV, 200 μA and 300 ms exposure time to obtain a 20 μm image resolution. As seen from sagittal, horizontal, and coronal views, bone formed within the boundary line of the defects was considered to be new bone. Relevant reconstruction software was used to reconstruct image slices and quantify the volume of newly regenerated bone in skull defect separately.

2.11 Histological/immunohistochemical staining

All skull specimens were decalcified with 10% EDTA (E1171, Solarbio) for 2 months after Miro-CT scanning. Decalcification solution was replaced once every 3 days. And specimens went through routinely dehydration and paraffin embedding. Vertical slices (4 μm) parallel to the long axis of the head were cut out from paraffin blocks, and then HE and Masson's trichrome staining were performed. In order to evaluate the protein expression level, the sections were incubated with corresponding antibodies (ALP, OC, IL-6, and TNF-α). Three sections were randomly selected from each group, and the positive staining of ALP, OC, IL-6, and TNF-α were observed on an Eclipse CI microscope (Nikon, Japan). Images of the stained tissue samples were taken at 400X and quantified using the Image Pro-Plus program. The positive staining was expressed as percentage of the positive area.

2.12 Statistics

The results are showed as means ± SDs. A value of P value < 0.05 was statistically significant. SPSS software version 17.0 was used to analyze datum. GraphPad Prism version 7.0 was used to constructe graphs.

3 Results

After euthanasia, the skulls of all rats were removed for further evaluation at 4^{th} week and 8^{th} week, respectively. No complications such as wound infection occurred during the experiment.

3.1 Characterization of scaffold

In order to apply scaffold in calvarial defect for bone regeneration, porous scaffold (Fig. 2a) was prepared and

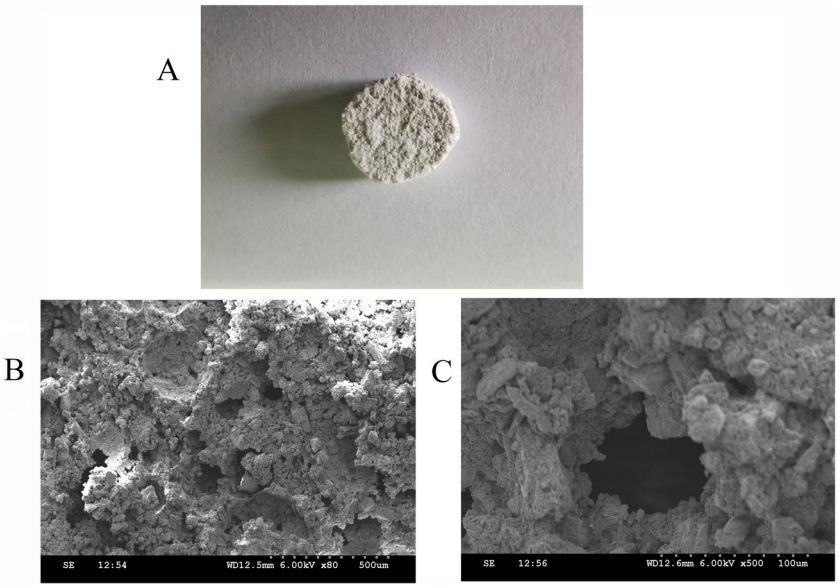

Fig. 2 Optical photographs of scaffold (**a**), SEM micrograph obtained from the surface of prepared scaffold at low (**b**) and higher magnification (**c**)

observed the characterization of the scaffold by SEM (Fig. 2b, c). SEM analysis showed that the mean pore diameter of the scaffold was about 150 µm with a range of 50–200 µm. And porosity of the scaffold was ~27.4%, which contributed to help BMSCs settle in scaffold. The prepared scaffolds were analyzed by XRD, and the results are shown in Fig. 3a. The main diffraction peaks of CSD/CSH and calcium carbonate and the characteristic diffraction peaks for bone-like apatite appeared. The existence of OS in scaffold was confirmed by FT-IR (Fig. 3b). The internal vibration modes of the CO_3^{2-} ions, 712, 700–877, 844–1082, and 1416 cm^{-1}, confirmed the existence of the carbonate ions. The strong IR band detected at 1796 cm^{-1} could also be attributed to the C=O groups of the carbonate ions. The element list analysis of XRF for the scaffold showed that the total proportion of calcium and oxygen were 95.95%, and it also contained sodium, iron, and other elements (Fig. 3c).

3.2 Ca^{2+} Release and pH in SBF of the scaffold

Figure 4 showed the changes in the calcium ion concentration and pH values of the SBF solution after SBF soaking. It can be observed that the scaffold could release calcium ions continuously in Fig. 4a and show an alkaline to acidic pH transition in Fig. 4b.

3.3 BMSCs' implantation to scaffold in vitro

ALP activity and OC of BMSCs were determined by ELISA at the fourth and eighth day. The ALP activity of group II, containing scaffold with BMSCs suspension, PRP and thrombin, was higher than group I ($P < 0.05$, Fig. 5). So PRP promoted BMSCs, on scaffold, osteogenic differentiation in vitro. Due to the lack of BMSCs in the group III and IV, osteogenic differentiation could not be initiated and ALP was almost not expressed in the two groups (Fig. 5). It is worth noting that OC was an indicator of late expression of osteogenic differentiation. Thus, the expression of OC was not detectable on day 4 or 8.

3.4 BMSCs' proliferation assay in vitro

The MTT assay data of BMSCs showed that the relative cell number (value of OD) of BMSCs+PRP group increased significantly compared to BMSCs group ($P < 0.05$, Fig. 6), which revealed PRP could promote BMSCs proliferation in vitro.

3.5 X-ray analysis

After the defect was created in the skull bone, X-ray imaging and analysis were performed to identify the position of the defect and the healing of the defect area at 4th and 8th week, respectively. As shown on the X-ray images, the bone regeneration began at the border of all bone defects and the initial skull defect area gradually decreased with time (Fig. 7). In particular, the healing of the defect area at 4th week showed significantly faster bone regeneration than that at 8th week, and the area of skull defect in each group was decreased in varying degrees. The Scaffold + PRP + BMSCs group showed the smallest defect area of skull among the experimental groups (Fig. 7b, $P < 0.05$), verifying that PRP in scaffold possessed an excellent ability of osteogenesis induced. What's more, due to the presence of PRP + BMSCs in scaffold, the area of skull defect decreased significantly compared to other treatments. In addition, the area of bone defect treated with Scaffold + PRP

A

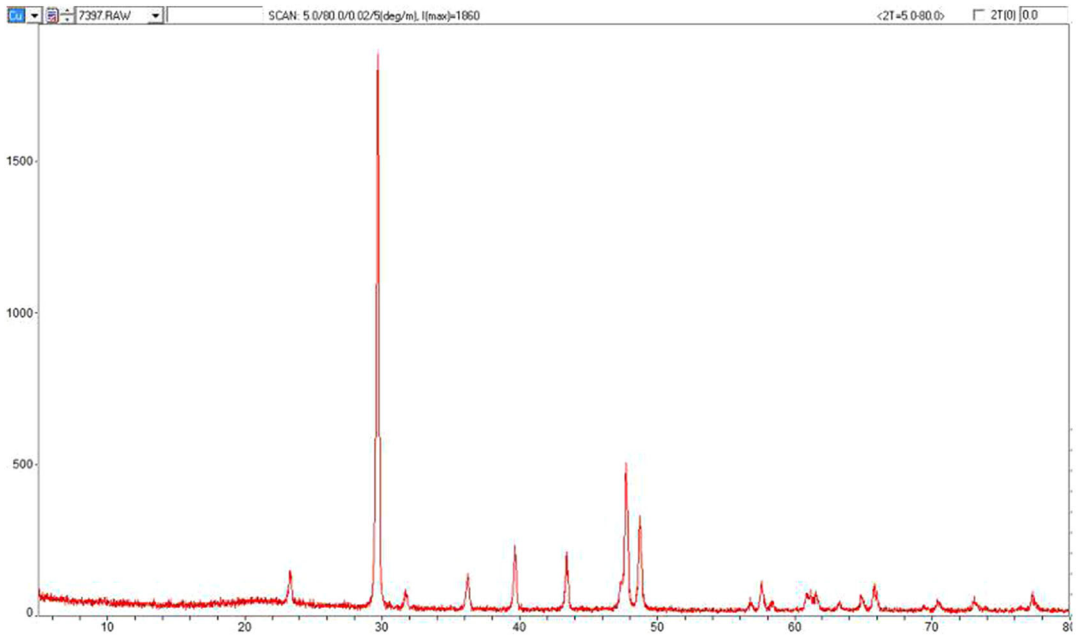

B

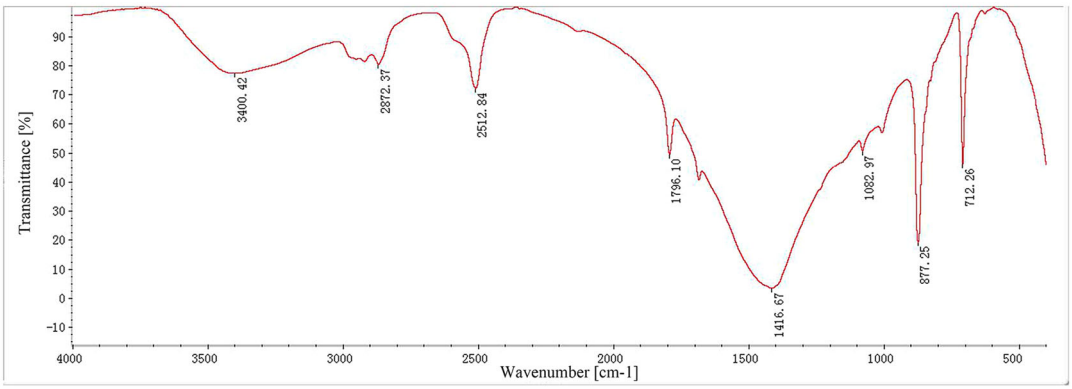

C

Analyte	Result	Proc-Calc	Line	Net Int.	BG Int.
Ca	63.7069 %	Quant.-FP	CaKa	3082.562	6.404
O	32.2480 %	Quant.-FP	O Ka	0.965	0.217
C	1.8449 %	Quant.-FP	C Ka	0.553	0.385
Mg	0.6642 %	Quant.-FP	MgKa	2.877	0.215
Na	0.4893 %	Quant.-FP	NaKa	0.781	0.062
Si	0.2600 %	Quant.-FP	SiKa	4.563	0.072
Sr	0.2445 %	Quant.-FP	SrKa	29.071	9.770
S	0.1447 %	Quant.-FP	S Ka	6.922	0.472
Al	0.1132 %	Quant.-FP	AlKa	1.320	0.175
Fe	0.1039 %	Quant.-FP	FeKa	1.925	0.414
P	0.0870 %	Quant.-FP	P Ka	4.272	0.453
Cl	0.0526 %	Quant.-FP	ClKa	1.125	0.992
K	0.0407 %	Quant.-FP	K Ka	3.032	1.264

Fig. 3 **a** XRD patterns of the scaffold; **b** FT-IR of the scaffold; **c** XRF element list analysis of the scaffold

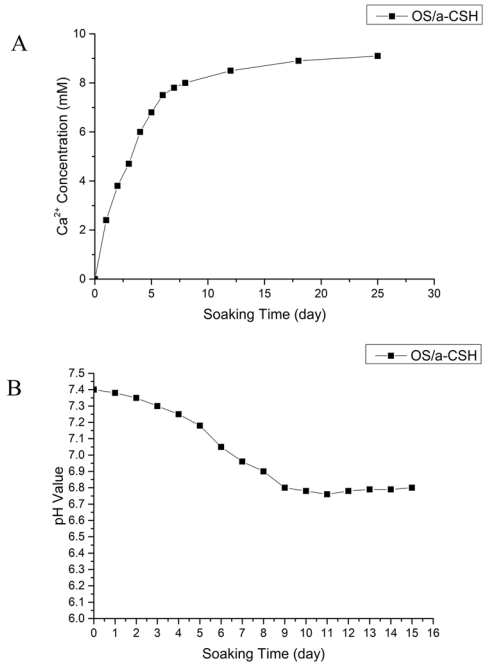

Fig. 4 Dependent of Ca^{2+} concentration (**a**) and the pH value (**b**) in the SBF solution of α-CSH/OS scaffold during soaking time

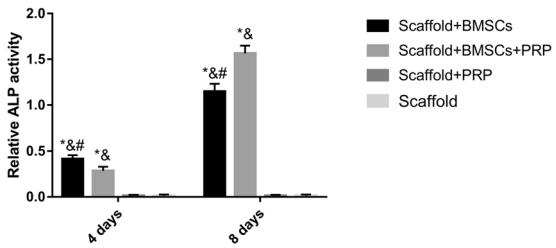

Fig. 5 ALP activity of each experimental group at different time. *$P <$ 0.05 as compared to group scaffold, &$P < 0.05$ as compared to group Scaffold+PRP, #$P < 0.05$ as compared to group Scaffold + BMSCs + PRP

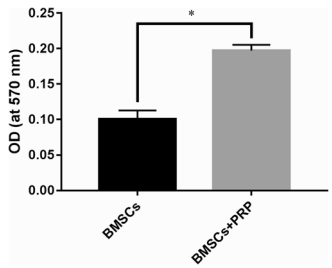

Fig. 6 Proliferation of BMSCs under different culture conditions. *Statistical significance was considered to be $P < 0.05$

was smaller than that in animals treated with scaffold or control (Fig. 7b, $P < 0.001$). The degree of remaining area of calvarial bone defect was different between scaffold group and control group, but the difference had no statistical significance (Fig. 7b, $P > 0.05$).

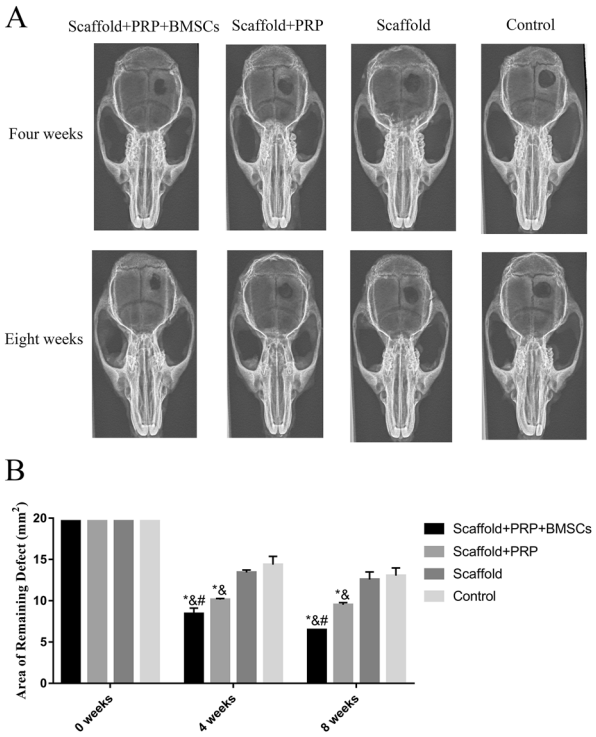

Fig. 7 **a** Scaffolds were treated after skull surgery. Samples were collected at 4 or 8 weeks and radiographs were taken to analyze the repairation of skull defects. **b** X-ray detection. The area of the remaining defect zones was measured in the radiographs using image pro-plus6.0 (Media Cybernetics, Inc., MD, USA). *$P < 0.05$ as compared to group control, & $P < 0.05$ as compared to group scaffold, #$P < 0.05$ as compared to group Scaffold+PRP. $n = 4$/group

3.6 Micro-CT analysis

At 8 weeks after operation, the formation of new bone was detected by Micro-CT. To certain extent, different quantities of new bone were formed in the all experimental groups (Fig. 8a). For the 8th week postoperative time point, the Scaffold + PRP + BMSCs group ($1.71 \pm 0.30\ mm^3$) showed the highest volume of newly regenerated bone, which was statistically significant (Fig. 8b, $P < 0.05$). During the same period, the newly regenerated bone volume of the animals treated with Scaffold+PRP + PRP ($1.25 \pm 0.10\ mm^3$) was larger than that in the scaffold group ($0.87 \pm 0.08\ mm^3$) and the control group ($0.83 \pm 0.02\ mm^3$), with these differences being significant (Fig. 8b, $P < 0.05$). However, there was no significant difference in the volume of newly formed bone at the implantation sites between the scaffold group and the control group ($0.87 \pm 0.08\ mm^3$ VS $0.83 \pm 0.02\ mm^3$, $P = 0.734$, Fig. 8b).

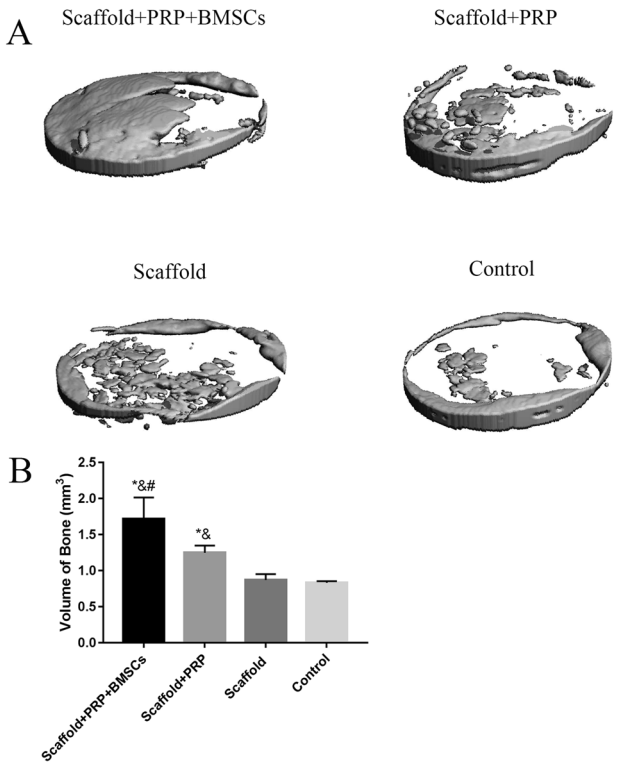

Fig. 8 **a** Three-dimensional reconstructed of calvarial defect calvarial defect at 8 weeks after craniotomy. **b** The volume of new bone within defect. $^{*}P < 0.05$ as compared to group control, & $P < 0.05$ as compared to group scaffold, # $P < 0.05$ as compared to group Scaffold +PRP. $n = 4$/group

3.7 HE staining and immunohistochemistry

Histological analysis at 8 weeks after surgery also confirmed the changes in the repair of calvarial bone defect defects. HE staining confirmed that all groups had different degrees of bone regeneration in calvarial defects (Fig. 9a). The Scaffold+PRP + BMSCs group and the Scaffold + PRP group showed more newly regenerated bone at the defect sites than scaffold group and control group (Fig. 9a). And the largest bone formation was shown in the Scaffold + PRP + BMSCs group in all experimental groups (Fig. 9a) and grew from the edge of defect toward the center, which suggested combined treatment of scaffold, PRP, and BMSCs contributed to improve bone formation. In Scaffold + PRP group, newly regenerated bone and dense fibrous connective tissues almost filled more than half of the bone defect. Little bone formation was observed and most of the defect areas were covered by fibroid tissues in scaffold group and control group.

The immunohistochemistry staining for osteogenic marker proteins ALP and OC revealed that the positive staining being detected was the highest in the Scaffold + PRP + BMSCs group ($P < 0.05$) (Fig. 9b, c). The expression of ALP and OC in the Scaffold + PRP group was significantly higher than that in scaffold group and control group ($P < 0.05$, Fig. 9b, c). In addition, positive brown staining was observed in scaffold group and control group, but no statistical difference was found between them ($P > 0.05$). The immunohistochemistry staining for inflammatory markers IL-6 and TNF-α showed that the positive expressions in control group were lowest in all groups ($P < 0.05$, Fig. 9d, e). In groups Scaffold + PRP + BMSCs, Scaffold+PRP and scaffold, the positive staining of IL-6 was the most obvious in the Scaffold + PRP group and the positive staining of TNF-α was the most obvious in the scaffold group. But no significant difference was found among the three groups ($P > 0.05$).

3.8 Masson staining

In order to detect collagen fibrils which often appeared in the process of osteogenic differentiation, we used Masson trichrome staining to evaluate newly regenerated collagen stained in blue in fibrous connective tissues (Fig. 10a). The blue dye indicated collagen fibrils and the red dye indicated muscle fiber or erythrocyte. Scaffold + PRP + BMSCs group showed the highest expression of collagen fibrils among the experimental groups (Fig. 10b, $P < 0.05$). Blue staining area occupied almost all new bone and just a little amount of red-stained muscle fiber was observed in Scaffold + PRP + BMSCs group. The expression of collagen fibrils in Scaffold + PRP group was $38.72 \pm 5.11\%$, which was obviously higher than that of scaffold group and the control group ($P < 0.05$, Fig. 10b). And a small amount of red stained areas was observed in some blue- stained new bone in Scaffold+PRP group (Fig. 10a). The expression of collagen fibrils in control group ($14.19 \pm 2.53\%$) was less than that in scaffold group ($23.22 \pm 2.35\%$). However, no statistical difference was found between them ($P = 0.078$, Fig. 10b).

4 Discussion

Skull defects are resultant from surgical procedures, trauma and other tumor removals. The reparation of skull defect requires autogenous bone graft transplantation, which is identified as the "gold standard" for the treatment of bone defects. However, some conditions limited the application of bone grafting technology such as donor site morbidity and the limited supply of bone available for transplantation [26]. To get rid of these limitations, a great deal of scaffolds is the subject of intense current research efforts and has been developed for the repairation of cranial defects. Scaffolds combinging artificially synthesized material and natural biomineral hold promising potential for repair of bone defect, which not only met the demand of bone

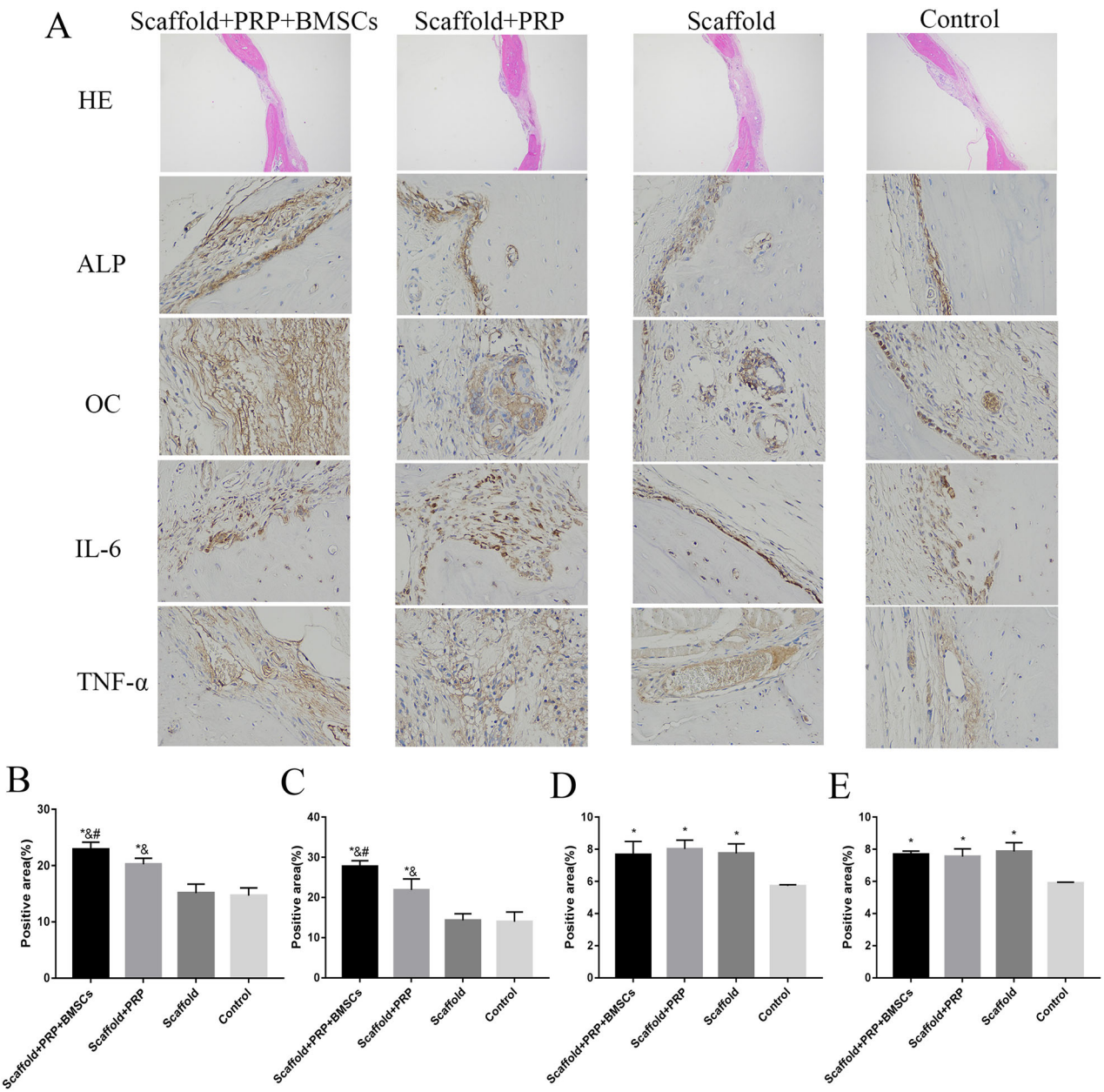

Fig. 9 **a** HE staining and immunohistochemical assay for ALP, OC, IL-6, and TNF-α expression in each group to observe osteogenesis and inflammation in calvarial defect. The brown color represents positive staining. **b** Positive area of ALP. **c** Positive area of OC, **d** Positive area of IL-6, **e** Positive area of TNF-α. *$P < 0.05$ as compared to group control, & $P < 0.05$ as compared to group scaffold, #$P < 0.05$ as compared to group scaffold+PRP. $n = 4$/group

transplantation, but also greatly increased the quantity and quality of osteogenesis in a short time [27–30].

We fabricated bioengineering scaffold, OS with α-CSH as scaffold, PRP as the provider of growth factors and BMSCs as seed cells, on healing critical-sized bone defects. And our results demonstrated the efficiency of this bioengineering scaffold in bone regeneration, and emphasized the potential ability to employ bioengineering scaffold for bone defect repairation. The porosity of the bioengineering scaffold is about 27.4%, and the average pore size is 150 μM, which was beneficial to the attachment, proliferation, division and differentiation of bone marrow mesenchymal stem cells and promote bone formation within the scaffold. In addition, the micro-pore structure of the scaffold could make the PRP and Ca^{2+} in the bioengineering scaffold continuously and slowly release to the edge of the defect and speed up the repair of bone defect. What's more, the porous structure of such scaffolds enhanced osseointegration allowing for new bone tissue growth into the pores and improved osteoconduction [31]. Kim et al.

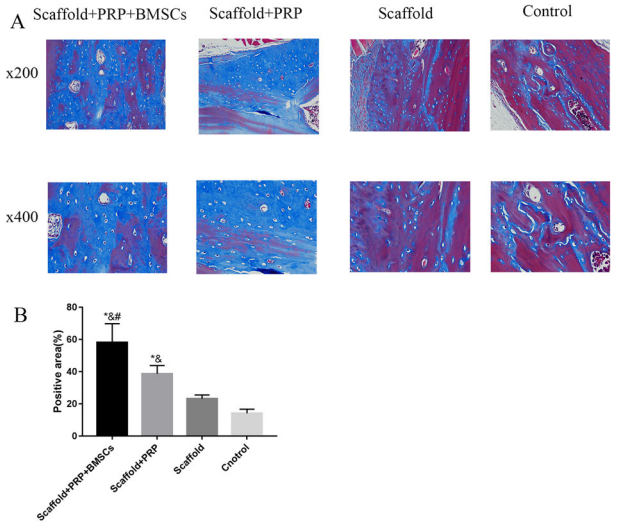

Fig. 10 **a** Microphotograph at week 8 after the surgical operation in experimental site. Masson staining. X200 and X400. **b** positive area of Masson. The blue color represents positive staining. X200

[32] pointed out that the higher the porosity, the more conducive to the growth of new bone. The transport of nutrients could be completed when the pore diameter of the porous scaffold was more than 20 μM, and the minimum pore diameter for cell adhesion and tissue growth was 100 μM. According to the results of the previous study [32], the pore size distribution of the porous scaffold materials prepared in this study can fully meet the requirements of bone tissue engineering for the porosity and pore size distribution of the scaffold materials.

Degradability is another important aspect to consider in evaluating implanted biomaterials, which is determined by the chemical structure and the physical characteristics of materials. One of the main challenges faced by pure α-CSH is the material's rapid rate of degradation, which cannot match the rate of bone regeneration. In our study, the α-CSH/OS composites presented a significantly delayed degradation rate compared to the degradation rate of pure α-CSH. The delayed degradation rate is attributed to the fact that the additive OS particles exhibit significantly low solubility. Either the embedded OS particles on the surface of CSD crystals or free OS particles among α-CSH particles could retard the penetration of SBF solution and reduce their degree of contact. Moreover, the presence of OS particles could provide a better microenvironment around the implantation location due to the chemical stability and weak ionization of carbonic acid molecules. Moreover, a solution with higher pH might facilitate the acid exudation of pure α-CSH in clinic applications [33]. Duplat et al. [34] observed that the degradation of OS was mainly based on physicochemical factors, whereas living cells mediating in an absorbing manner played limited role on the degradation. Duplat et al. [35] also indicated that the high mineral content of OS and calcium release into resorption lacunae would trigger the inhibition of osteoclast activity [36, 37]. Our results also indicate that Ca^{2+} ions are released during soaking in SBF. Maeno et al. [38] concluded that $2-4$ mM Ca^{2+} is suitable for the proliferation and survival of osteoblasts, whereas slightly higher concentrations ($6-8$ mM) favor osteoblast differentiation and matrix mineralization in both two- and three-dimensional cultures. Higher concentrations (410 mM) are cytotoxic. Figure 4 demonstrates that the Ca^{2+} release of the α-CSH/OS composites occurred more smoothly during the degradation period and more closely approached the most suitable Ca^{2+} concentration ($6-8$ mM) after 1 week. To summarize, the degradation rate and microenvironment of the α-CSH/OS composite pastes was ameliorated by the addition of OS. We did experiments in vitro and in vivo to further evaluate the effect of bioengineering scaffold on the repair of bone defect.

ALP was a cell membrane-associated enzyme, which was the most widely recognized marker in the early stage of osteoblast differentiation [39]. In our vitro experiment, when OS scaffold conbined with BMSCs, PRP and thrombin, the results presented an obviously higher ALP activity compared with other experimental groups at 4 and 8 day, which demonstrated that PRP is beneficial to promote osteogenic differentiation of BMSCs in vitro. This fnding was consistent with Roubelakis et al.'s result [40]. Meheux et al. [41] and Wang et al. [42] also pointed out that PRP had been widely used in various clinical procedures due to its high concentration of growth factors and bioactive proteins (such as platelet derived growth factor, transforming growth factor-β, bone morphogenetic protein 2 and insulin-like growth factor) that influence the healing of bone injuries, which further supports our result that the positive role of PRP in osteogenic differentiation in vitro. In addition, the proliferation of BMSCs in vitro was also carried out. The proliferation of BMSCs in the experimental group was compared by adding PRP or not. MTT assay demonstrated that the cell proliferation in PRP group was obviously higher than that in non-PRP group, which was inclined toward promoting the cellular proliferation of BMSCs. This tesult further proved the proliferation and osteogenic induction of PRP in bone defect repair and provided theoretical support for the previous study [40]. OC participated in the control of mineralization process and was the characteristic of osteoblast cell maturation, which appeared at a late stage of osteogenic differentiation [41, 42]. The expression of OC was not detectable by the ELISA determination at day 4 and 8. We believed that this result was mainly due to the short induction time of osteogenesis and the incomplete osteogenesis process.

For exploring its potential clinical applications, the ability of bioengineering scaffold to repair a critical sized skull defect was studied in vivo [43]. When over the critical size, bone defects lose the spontaneously regenerative capacity to heal without intervention. For the weak blood supply and poor bone regeneration, rat calvarial defect model was extensively used in bone graft researches [44]. A 5 mm in diameter is the most widely used size in modeling rat calvarial defects [45]. 5 mm defect would not damage calvarial bone structural stabilization. And with the support by dura and scalp, bone graft substitutes could be placed into the defect space without extra fixation [46]. Therefore, on the basis of previously similar studies [47], we chose the SD rat calvarial defect model with 5 mm in diameter and 8 weeks as the terminal of our animal study.

Compared to group II (scaffold + PRP), group III (scaffold) and group IV (blank control), the results of X-ray imaging and Micro-CT showed the benefit of delivering PRP, yielding bone regeneration and repairing the area of skull defect significantly exceeding that of scaffold and control. What's more, these results showed the benefit of co-delivering BMSCs with PRP, yielding new bone and repairing the area of skull defect greater than these of Scaffold+PRP, scaffold and control. The result indicates that BMSCs and the growth factors in PRP have large effects on nearly every stage of bone defect healing. Previous studies also found that transplanted stem cells were able to participate in and contribute to osteogenesis [48]. For example, in vitro osteogenic induction of hBMSCs seeding on β-TCP ceramic significantly enhanced ectopic bone formation [49]. In addition, adipose-derived stem cells (ACS) accelerated bone regeneration, although ACS seemed to be inferior to BMSCs in osteogenic potential [50]. This further indicates that the implantation of BMSCs on the scaffolds can accelerate the repair of bone defects and promote the formation of new bone. In 8 weeks after surgery, most substitute material in defect area was absorbed and residues became hard to observe in Micro-CT and histologic sections. Immunohistochemistry staining against ALP and OC demonstrated greater osteogenic differentiation and mineralization in Scaffold + PRP + BMSCs group compared to remaining groups.

Scaffold was made of OS and α-CSH according to a certain proportion. Oyster shells (OS) has low cost, wide availability and natural biological origin, which contains crystal structure and composition similar to human bone so its application as the raw material for bone tissue engineering is promising [51]. And OS is mainly composed of calcium carbonate biomineral, which is also considered to be an ideal bone substitute material [52]. Mount et al. [8] found that the biomineralization process of OS was similar to osteogenesis in the human body. When meeting water, α-CSH will turned into CSD and solidify in few minutes, which has been used to produce calcium sulfate cement for bone augmentation and bone graft substitutes [15]. And this process is slightly exothermic. Some previous studies had shown that calcium sulfate was an outstanding bone substitute due to good biodegradability, biocompatibility, and osteoconductivity [53–56]. In addition, Kim et al. [57] found that calcium sulfate had potentially osteoinductive-like differentiation of BMSCs into osteoblasts. Calcium sulfate promoted bone regeneration mechanism might be to maintain high levels of extracellular calcium ions [58, 59]. Therefore, the two materials were mixed in a certain proportion to provide the corresponding calcium ion and bridge effect for osteogenesis.

Yoshimi et al. [60] and Man et al. [61] had investigated the causes and mechanisms of combined delivering of BMSCs and PRP to enhance bone regeneration, which further supported our findings. As the source of progenitors for osteoblasts, BMSCs acted seed cells in the repair of bone defects and played a significant role in the homeostasis of bone and bone marrow, which regulated the osteogenic differentiation and bone tissue regeneration process [48]. PRP was confirmed to promote bone regeneration [62–65]. Platelet 100 × 104/μl in PRP had a good effect on inducing osteogenesis [66]. And it provided BMSCs with growth factors such as IGF, PDGF, TGF-β, VEGF, and so on [60, 61, 67]. A large number of growth factors in PRP could activate intracellular signal transduction, which promoted the proliferation, differentiation, collagen fiber synthesis and tissue matrix formation of BMSCs [61, 67]. All in all, scaffold serve as bridge and release calcium ions, stem cells act as seed cells, and PRP provides growth factors. The combined action of them can provide good osteogenesis and effectively promote bone healing.

What's more, slight inflammatory reaction was observed in all the four groups. The immunohistochemistry staining for inflammatory markers IL-6 and TNF-α showed that the positive expressions in Scaffold + PRP + BMSCs group, Scaffold + PRP group and scaffold group were higher than these in control group ($P < 0.05$). However, no significant difference was found among the three experimental groups. However, the group I had the best bone healing and the largest new bone mass, while the control group had poor healing. This result suggested that slight inflammatory stimulation could promote bone healing and new bone formation. Li et al. [68] found that MG63 cells grown on MSC-CM pre-treated with IFN-g and TNF-α exhibit superior biological characteristics compared with those grown on pre-treated media with no inflammatory cytokines or a single inflammatory cytokine. When cultured in MSC-CM pretreated with both IFN-g and TNF-α, the proliferation and migration of MG63 cells were significantly promoted, thereby contributing to the osteogenesis transformation from the proliferation phase to the

differentiation phase. Hess et al. [69] had proved that TNF-α promoted osteogenic differentiation of human mesenchymal stem cells by triggering the NF-kappaB signaling pathway. These studies further support our findings that slight inflammatory stimulation could effectively promote osteogenesis and bone healing [68, 69]. As for other inflammatory pathways and the effect of inflammatory level on osteogenesis, we will continue to explore in future experiments. In this study, the combined effects of these factors contributed to increase the absorption of scaffolds, enhance the regeneration of new bone and repair of bone defects. Overall, the combination of scaffold with PRP and BMSCs is an effective approach for bone regeneration and repair. And this kind of bioengineering scaffold can be applied as a new type of bone graft substitutes by rat calvarial bone defects repairing experiment.

5 Conclusions

Scaffold, OS with α-CSH, is porous and absorbable, which combines the self-setting ability of calcium sulfate and the bioactivity of OS, maintains high levels of extracellular calcium ions and provides bridge effect for osteogenesis. As the source of progenitors for osteoblasts, BMSCs regulated the osteogenic differentiation and bone tissue regeneration process. PRP provided BMSCs with growth factors such as IGF, PDGF, TGF-β and VEGF, and activate intracellular signal transduction, which promoted the proliferation, differentiation, collagen fiber synthesis and tissue matrix formation of BMSCs. Slight inflammatory stimulation could effectively promote osteogenesis and bone healing. In conclusion, the combined action of them can provide good osteogenesis and effectively promoted the bone healing of critical-size calvarial defects in rats. The resultant composite bioengineering scaffold is very promising candidates for facilitating osteoanagenesis in clinic treatment.

Acknowledgements This study was supported by Department of Health of Zhejiang Province (No. 2016KYB196) and Science and Technology Department of Zhejiang Province (No. 2017C37125).

Compliance with ethical standards

Conflict of interest The authors declare that they have no conflict of interest.

Ethics The experiments described in this study were approved by the Ethics Committee of the Second Affiliated Hospital of Wenzhou Medical University.

Publisher's note Springer Nature remains neutral with regard to jurisdictional claims in published maps and institutional affiliations.

References

1. Haines NM, Lack WD, Seymour RB, Bosse MJ. Defining the lower limit of a "critical bone defect" in open diaphyseal tibial fractures. J Orthop Trauma. 2016;30:e158–63.
2. Roffi A, Di Matteo B, Krishnakumar GS, Kon E, Filardo G. Platelet-rich plasma for the treatment of bone defects: from preclinical rational to evidence in the clinical practice. A systematic review. Int Orthopaedics. 2017;41:221–37.
3. Granel H, Bossard C, Nucke L, Wauquier F, Rochefort GY, Guicheux J, et al. Optimized bioactive glass: the quest for the bony graft. Adv Healthcare Mater. 2019;8:e1801542.
4. Giannoudis PV, Einhorn TA, Marsh D. Fracture healing: the diamond concept. Injury. 2007;null:S3–6.
5. Hutmacher DW, Schantz JT, Lam CXF, Tan KC, Lim TC. State of the art and future directions of scaffold-based bone engineering from a biomaterials perspective. J Tissue Eng Regen Med. 2007;1:245–60.
6. Henkel J, Woodruff MA, Epari DR, Steck R, Glatt V, Dickinson IC, et al. Bone regeneration based on tissue engineering conceptions - a 21st century perspective. Bone Res. 2013;1:216–48.
7. Lee YH, Islam SMdA, Hong SJ, Cho KM, Math RK, Heo JY, et al. Composted oyster shell as lime fertilizer is more effective than fresh oyster shell. Biosci Biotechnol Biochem. 2010;74:1517–21.
8. Mount AS, Wheeler AP, Paradkar RP, Snider D. Hemocyte-mediated shell mineralization in the eastern oyster. Science. 2004;304:297–300.
9. Gerhard EM, Wang W, Li C, Guo J, Ozbolat IT, Rahn KM, et al. Design strategies and applications of nacre-based biomaterials. Acta Biomater. 2017;54:21–34.
10. Atlan G, Balmain N, Berland S, Vidal B, Lopez E. Reconstruction of human maxillary defects with nacre powder: histological evidence for bone regeneration. Comptes rendus de l'Academie des sciences Serie III, Sciences de la vie. 1997;320:253–8.
11. Lopez E, Vidal B, Berland S, Camprasse S, Camprasse G, Silve C. Demonstration of the capacity of nacre to induce bone formation by human osteoblasts maintained in vitro. Tissue Cell. 1992;24:667–79.
12. Green DW, Kwon H-J, Jung H-S. Osteogenic potency of nacre on human mesenchymal stem cells. Mol Cells. 2015;38:267–72.
13. Lee GH, Khoury JG, Bell J-E, Buckwalter JA. Adverse reactions to OsteoSet bone graft substitute, the incidence in a consecutive series. The Lowa Orthopaedic J. 2002;22:35–8.
14. Ferguson JY, Dudareva M, Riley ND, Stubbs D, Atkins BL, McNally MA. The use of a biodegradable antibiotic-loaded calcium sulphate carrier containing tobramycin for the treatment of chronic osteomyelitis: a series of 195 cases. The Bone Joint J. 2014;null:829–36.
15. Coetzee AS. Regeneration of bone in the presence of calcium sulfate. Arch Otolaryngology (Chicago, Ill: 1960). 1980;106:405–9.
16. Khan Y, Yaszemski MJ, Mikos AG, Laurencin CT. Tissue engineering of bone: material and matrix considerations. J Bone Joint Surg Am Vol. 2008;null:36–42.
17. Lang S, Loibl M, Herrmann M. Platelet-rich plasma in tissue engineering: hype and hope. Eur Surg Res. 2018;59:265–75.
18. Ahmed HH, Rashed LA, Mahfouz S, Hussein RE, Alkaffas M, Mostafa S, et al. Can mesenchymal stem cells pretreated with platelet-rich plasma modulate tissue remodeling in a rat with burned skin? Biochem Cell Biol. 2017;95:537–48.
19. Smith SE, Roukis TS. Bone and wound healing augmentation with platelet-rich plasma. Clin Podiatr Med Surg. 2009;26:559–88.

20. Kim YS, Lee HJ, Yeo JE, Kim YIL, Choi YJ, Koh YG. Isolation and characterization of human mesenchymal stem cells derived from synovial fluid in patients with osteochondral lesion of the talus. Am J Sports Med. 2015;43:399–406.
21. Quarto R, Mastrogiacomo M, Cancedda R, Kutepov SM, Mukhachev V, Lavroukov A, et al. Repair of large bone defects with the use of autologous bone marrow stromal cells. N Engl J Med. 2001;344:385.
22. Johari N, Fathi MH, Golozar MA. The effect of fluorine content on the mechanical properties of poly (ε-caprolactone)/nano-fluoridated hydroxyapatite scaffold for bone-tissue engineering. Ceram Int. 2011;37:3247–51.
23. Zhang R, Ma PX. Poly(alpha-hydroxyl acids)/hydroxyapatite porous composites for bone-tissue engineering. I. Preparation and morphology. J Biomed Mater Res. 2015;44:446–55.
24. Kokubo T, Takadama H. How useful is SBF in predicting in vivo bone bioactivity? Biomaterials. 2006;27:2907–15.
25. Chen Y, Xu J, Huang Z, Yu M, Zhang Y, Chen H, et al. An innovative approach for enhancing bone defect healing using PLGA scaffolds seeded with extracorporeal-shock-wave-treated bone marrow mesenchymal stem cells (BMSCs). Sci Reports. 2017;7:44130.
26. Scaglione S, Lazzarini E, Ilengo C, Quarto R. A composite material model for improved bone formation. J Tissue Eng Regenerative Med. 2010;4:505–13.
27. Johari B, Ahmadzadehzarajabad M, Azami M, Kazemi M, Soleimani M, Kargozar S, et al. Repair of rat critical size calvarial defect using osteoblast-like and umbilical vein endothelial cells seeded in gelatin/hydroxyapatite scaffolds. J Biomed Mater Res Part A. 2016;104:1770–8.
28. Zhou D, Qi C, Chen Y-X, Zhu Y-J, Sun T-W, Chen F, et al. Comparative study of porous hydroxyapatite/chitosan and whitlockite/chitosan scaffolds for bone regeneration in calvarial defects. Int J Nanomed. 2017;12:2673–87.
29. Liang P, Zheng J, Zhang Z, Hou Y, Wang J, Zhang C, et al. Bioactive 3D scaffolds self-assembled from phosphorylated mimicking peptide amphiphiles to enhance osteogenesis. J Biomater Sci Polymer Ed. 2019;30:34–48.
30. Coringa R, de Sousa EM, Botelho JN, Diniz RS, de Sa JC, da Cruz M, et al. Bone substitute made from a Brazilian oyster shell functions as a fast stimulator for bone-forming cells in an animal model. PLoS ONE. 2018;13:e0198697.
31. Stoppato M, Carletti E, Sidarovich V, Quattrone A, Unger RE, Kirkpatrick CJ, et al. Influence of scaffold pore size on collagen I development: a new in vitro evaluation perspective. J Bioactive Compatible Polymers. 2013;28:16–32.
32. Kim HW, Shin SY, Kim HE, Lee YM, Chung CP, Lee HH, et al. Bone formation on the apatite-coated zirconia porous scaffolds within a rabbit calvarial defect. J Biomater Appl. 2008;22:485–504.
33. Fernandez E, Vlad MD, Gel MM, Lopez J, Torres R, Cauich JV, et al. Modulation of porosity in apatitic cements by the use of alpha-tricalcium phosphate-calcium sulphate dihydrate mixtures. Biomaterials. 2005;26:3395–404.
34. Duplat D, Chabadel A, Gallet M, Berland S, Bedouet L, Rousseau M, et al. The in vitro osteoclastic degradation of nacre. Biomaterials. 2007;28:2155–62.
35. Duplat D, Gallet M, Berland S, Marie A, Dubost L, Rousseau M, et al. The effect of molecules in mother-of-pearl on the decrease in bone resorption through the inhibition of osteoclast cathepsin K. Biomaterials. 2007;28:4769–78.
36. Lorget F, Kamel S, Mentaverri R, Wattel A, Naassila M, Maamer M, et al. High extracellular calcium concentrations directly stimulate osteoclast apoptosis. Biochem Biophys Res Commun. 2000;268:899–903.
37. Miyauchi A, Hruska KA, Greenfield EM, Duncan R, Alvarez J, Barattolo R, et al. Osteoclast cytosolic calcium, regulated by voltage-gated calcium channels and extracellular calcium, controls podosome assembly and bone resorption. J Cell Biol. 1990;111:2543–52.
38. Maeno S, Niki Y, Matsumoto H, Morioka H, Yatabe T, Funayama A, et al. The effect of calcium ion concentration on osteoblast viability, proliferation and differentiation in monolayer and 3D culture. Biomaterials. 2005;26:4847–55.
39. Ducy P, Zhang R, Geoffroy VR, Ridall AL, Karsenty GR. Osf2/Cbfa1: a transcriptional activator of osteoblast differentiation. Cell. 1997;89:747–54.
40. Roubelakis MG, Trohatou O, Roubelakis A, Mili E, Kalaitzopoulos I, Papazoglou G, et al. Platelet-rich plasma (PRP) promotes fetal mesenchymal stem/stromal cell migration and wound healing process. Stem Cell Rev Reports. 2014;10:417–28.
41. Sun H, Feng K, Hu J, Soker S, Atala A, Ma PX. Osteogenic differentiation of human amniotic fluid-derived stem cells induced by bone morphogenetic protein-7 and enhanced by nanofibrous scaffolds. Biomaterials. 2010;31:1133–9.
42. Kasten P, Vogel J, Geiger F, Niemeyer P, Luginbühl R, Szalay K. Biomaterials SKJ. The effect of platelet-rich plasma on healing in critical-size long-bone defects. Biomaterials. 2008;29:3983–92.
43. Wang H, Zhao S, Xiao W, Cui X, Huang W, Rahaman MN, et al. Three-dimensional zinc incorporated borosilicate bioactive glass scaffolds for rodent critical-sized calvarial defects repair and regeneration. Colloids Surf B: Biointerfaces. 2015;130:149–56.
44. Liu M, Lv Y. Reconstructing bone with natural bone graft: a review of in vivo studies in bone defect animal model. Nanomaterials. 2018;8:1–19.
45. McGovern JA, Griffin M, Hutmacher DW. Animal models for bone tissue engineering and modelling disease. Dis Models Mech. 2018;11:1–14.
46. Gomes PS, Fernandes MH. Rodent models in bone-related research: the relevance of calvarial defects in the assessment of bone regeneration strategies. Lab Anim. 2011;45:14–24.
47. Yu X, Sun J, Hu Y, Gao Y, Xiao C, Liu S, et al. Overexpression of PLAP-1 in bone marrow stromal cells inhibits the rat critical-size skull defect repair. J Mol Histol. 2015;46:251–61.
48. El Tamer MK, Reis RL. Progenitor and stem cells for bone and cartilage regeneration. J Tissue Eng Regen Med. 2009;3:327–37.
49. Ye X, Yin X, Yang D, Tan J, Liu G. Ectopic bone regeneration by human bone marrow mononucleated cells, undifferentiated and osteogenically differentiated bone marrow mesenchymal stem cells in beta-tricalcium phosphate scaffolds. Tissue Eng Part C Methods. 2012;18:545–56.
50. Niemeyer P, Fechner K, Milz S, Richter W, Suedkamp NP, Mehlhorn AT, et al. Comparison of mesenchymal stem cells from bone marrow and adipose tissue for bone regeneration in a critical size defect of the sheep tibia and the influence of platelet-rich plasma. Biomaterials. 2010;31:3572–9.
51. Kazemi SY, Biparva P, Ashtiani E. Cerastoderma lamarcki shell as a natural, low cost and new adsorbent to removal of dye pollutant from aqueous solutions: equilibrium and kinetic studies. Ecological Eng. 2016;88:82–9.
52. Balmain J, Hannoyer B, Lopez E. Fourier transform infrared spectroscopy (FTIR) and X-ray diffraction analyses of mineral and organic matrix during heating of mother of pearl (nacre) from the shell of the mollusc Pinctada maxima. J Biomed Mater Res. 1999;48:749–54.
53. Beuerlein MJ, McKee MD. Calcium sulfates: what is the evidence? J Orthopaedic Trauma. 2010;24:S46–51.
54. Shen Y, Yang S, Liu J, Xu H, Shi Z, Lin Z, et al. Engineering scaffolds integrated with calcium sulfate and oyster shell for enhanced bone tissue regeneration. ACS Appl Mater Interfaces. 2014;6:12177–88.

55. Walsh WR, Morberg P, Yu Y, Yang JL, Haggard W, Sheath PC, et al. Response of a calcium sulfate bone graft substitute in a confined cancellous defect. Clin Orthopaedics Related Res. 2003;406:228–36.
56. Hammouche S, Khan W, Drouin H, Procter H, McNicholas M. Calcium salts bone regeneration scaffolds: a review article. Curr Stem Cell Res Therapy. 2012;7:336–46.
57. Kim YK, Lee JY, Kim SG, Lim SC. Guided bone regeneration using demineralized allogenic bone matrix with calcium sulfate: case series. J Adv Prosthodontics. 2013;5:167–71.
58. Kanatani M, Sugimoto T, Kanzawa M, Yano S, Chihara K. High extracellular calcium inhibits osteoclast-like cell formation by directly acting on the calcium-sensing receptor existing in osteoclast precursor cells. Biochem Biophys Res Commun. 1999;261:144–8.
59. Thomas MV, Puleo DA, Al-Sabbagh M. Calcium sulfate: a review. J Long-Term Eff Med implants. 2005;15:599–607.
60. Yoshimi R, Yamada Y, Ito K, Nakamura S, Abe A, Nagasaka T, et al. Self-assembling peptide nanofiber scaffolds, platelet-rich plasma, and mesenchymal stem cells for injectable bone regeneration with tissue engineering. J Craniofacial Surg. 2009;20:1523–30.
61. Man Y, Wang P, Guo Y, Xiang L, Yang Y, Qu Y, et al. Angiogenic and osteogenic potential of platelet-rich plasma and adipose-derived stem cell laden alginate microspheres. Biomaterials. 2012;33:8802–11.
62. Magesh DPU, Kumaravelu C, Maheshwari GU. Efficacy of PRP in the reconstruction of mandibular segmental defects using iliac bone grafts. J Maxillofacial Oral Surg. 2012;12:160–7.
63. Siebrecht MA, De Rooij PP, Arm DM, Olsson ML, Aspenberg P. Platelet concentrate increases bone ingrowth into porous hydroxyapatite. Orthopedics. 2002;25:169–72.
64. Thorwarth M, Wehrhan F, Schultze-Mosgau S, Wiltfang J, Schlegel KA. PRP modulates expression of bone matrix proteins in vivo without long-term effects on bone formation. Bone. 2006;38:30–40.
65. Weibrich G, Hansen T, Kleis W, Buch R, Hitzler WE. Effect of platelet concentration in platelet-rich plasma on peri-implant bone regeneration. Bone. 2004;34:665–71.
66. Yamakawa J, Hashimoto J, Takano M, Takagi M. The bone regeneration using bone marrow stromal cells with moderate concentration platelet-rich plasma in femoral segmental defect of rats. Open Orthopaedics J. 2017;11:1–11.
67. Intini G. The use of platelet-rich plasma in bone reconstruction therapy. Biomaterials. 2009;30:4956–66.
68. Li C, Li G, Liu M, Zhou T, Zhou H. Paracrine effect of inflammatory cytokine-activated bone marrow mesenchymal stem cells and its role in osteoblast function. J Biosci Bioeng. 2016;121:213–9.
69. Hess K, Ushmorov A, Fiedler J, Brenner RE, Wirth T. TNFalpha promotes osteogenic differentiation of human mesenchymal stem cells by triggering the NF-kappaB signaling pathway. Bone. 2009;45:367–76.